Multiparticle quantum walk: A dynamical probe of topological many-body excitations

Bogdan Ostahie,[1] Doru Sticlet,[2,*] Cătălin Pașcu Moca,[3,4] Balázs Dóra,[3,5] Miklós Antal Werner,[3,6] János K. Asbóth,[3,7] and Gergely Zaránd[3,6]

[1]*National Institute of Materials Physics, RO-077125 Bucharest-Magurele, Romania*
[2]*National Institute for R&D of Isotopic and Molecular Technologies, 67-103 Donat, RO-400293 Cluj-Napoca, Romania*
[3]*Department of Theoretical Physics, Institute of Physics, Budapest University of Technology and Economics, Műegyetem rakpart 3, H-1111 Budapest, Hungary*
[4]*Department of Physics, University of Oradea, RO-410087 Oradea, Romania*
[5]*MTA-BME Lendület Topology and Correlation Research Group, Műegyetem rakpart 3, H-1111 Budapest, Hungary*
[6]*MTA-BME Quantum Dynamics and Correlations Research Group, Műegyetem rakpart 3, H-1111 Budapest, Hungary*
[7]*Institute for Solid State Physics and Optics, Wigner Research Centre for Physics, P.O. Box 49, H-1525 Budapest, Hungary*

(Received 14 November 2022; revised 25 January 2023; accepted 6 July 2023; published 13 July 2023)

Recent experiments demonstrated that single-particle quantum walks can reveal the topological properties of single-particle states. Here, we generalize this picture to the many-body realm by focusing on multiparticle quantum walks of strongly interacting fermions. After injecting N particles with multiple flavors in the interacting SU(N) Su-Schrieffer-Heeger chain, their multiparticle continuous-time quantum walk is monitored by a variety of methods. We find that the many-body Berry phase in the N-body part of the spectrum signals a topological transition upon varying the dimerization, similarly to the single-particle case. This topological transition is captured by the single- and many-body mean chiral displacement during the quantum walk and remains present for strong interaction as well as for moderate disorder. Our predictions are well within experimental reach for cold atomic gases and can be used to detect the topological properties of many-body excitations through dynamical probes.

DOI: 10.1103/PhysRevB.108.035126

I. INTRODUCTION

Our conventional understanding of phase transitions associated with a symmetry breaking and the emergence of a local order parameter [1] has been extended with the advent of topological insulators [2,3]. Such materials are *not* characterized by a local order parameter and display various topological phases identified by topological invariants [4,5]. In noninteracting systems, topological invariants account for the topological character of single-particle wave functions and are accompanied by robust low-energy features at the boundaries of the system [6,7]. Not only are these useful in revealing the topological properties of matter, but also hold the promise to revolutionize quantum computation, quantum technologies, and spintronics [8–10].

While the study of noninteracting topological systems has advanced significantly in recent years, and the basic physics of noninteracting topological insulators is well understood by now, research into the analogous strongly correlated systems has progressed slowly [11,12], and it is rather unclear whether topology survives the presence of strong interactions [13]. Electron-electron interactions may in some situations be responsible for topological phase transitions, as it was demonstrated that a single quadratic band crossing is unstable with respect to topological insulating phases in the presence of interactions [14,15]. More generally, a mean-field decoupling of the interaction can result in an effective spin-orbit coupling, for instance, thus inducing a transition from a topologically trivial to a nontrivial phase [16–18]. Thus, understanding the topology of the ensuing phase and disentangling it from single-particle topological states is far from trivial.

It is therefore extremely important to establish ways for characterizing an interacting topological insulator [12,19]. The most likely candidate, which generalizes the underlying noninteracting Berry phase, would be the occurrence of a quantized many-body Berry phase [20–23]. Other proposals suggest a connection between topology and the degeneracy of the entanglement [24,25] or entropy itself [26]. However, testing any of these hypotheses experimentally in bulk systems is a challenging task.

A simple, experimentally appealing way to probe topology invokes the quench dynamics of quantum particles in single-particle quantum walks [27]. Recent experiments have revealed the presence of bound states at the interface of systems with different topological phases [28,29] and allow for the detection of topological invariants in cold atoms [30] or in nanophotonic topological lattice through the mean chiral displacement (MCD) [27,31,32], which measures the difference of the average occupations of the dimerized lattice in the long-time limit [see Eq. (5) for a concise definition]. So far, the MCD has been measured experimentally only in a noninteracting setup, by performing single-photon quantum walks in topological photonic lattices [27,32–34].

*doru.sticlet@itim-cj.ro

By now, experimental quantum walks have been implemented for trapped atoms and ions [35,36], photons [37–39], or spin impurities [40,41], and full control over the dynamics has been achieved. Furthermore, with recent advances in nanophotonics [42,43], quantum walks of correlated photons, and correlation effects in Bloch oscillations [44,45] in multiparticle quantum walks have already been realized. It is therefore interesting to explore whether the MCD is a suitable quantity to capture topology in the presence of strong interactions as well [46].

II. MODELS

A. Interacting SU(N) Su-Schrieffer-Heeger model

In the present paper we address this problem, and investigate the effect of interactions on the bulk states' topology in a multiparticle quantum walk setup. For that, we corroborate results on the Berry phase, computed using the many-body spectrum in a subspace of excited states with a reduced number of particles, and results on single-particle and many-body MCDs.

For the noninteracting SU(N) Su-Schrieffer-Heeger (SSH) model, the cases of N odd and even differ significantly, similarly to other spin models [47]. The Berry phase γ_B is marked by a jump of πN (modulo 2π) at the topological transition, therefore for even N, γ_B is unable to distinguish between the topological phases [48]. This is inherited in the interacting version of the model, where the many-body Berry phase defined below displays a jump π only for odd N, and can be used as an indicator of the topological transition. Nevertheless, the dynamically accessible single- and many-body MCDs identify correctly the topological phases for any number of flavors [49], are robust against moderate disorder, and serve as suitable measures to interrogate the bulk states' topology. For clarity, in this paper we mostly explore the simplest case, $N = 3$, where γ_B is also a good indicator. Results for the SU(2) SSH model are detailed in the Supplemental Material [49], where extensions to $N > 3$ are also considered.

The prototypical SU(N) SSH model [50] with an on-site Hubbard interaction is given by

$$H = \sum_{x=-L/2}^{L/2} \Bigg\{ -J \sum_{\alpha=1}^{N} [1 + (-1)^x \delta](c^\dagger_{x,\alpha} c_{x+1,\alpha} + \text{H.c.}) + U \sum_{1 \leqslant \alpha < \beta \leqslant N} c^\dagger_{x,\alpha} c_{x,\alpha} c^\dagger_{x,\beta} c_{x,\beta} \Bigg\}. \quad (1)$$

The first term in Eq. (1) accounts for the dimerized hopping with amplitudes $J_{1,2} = J(1 \pm \delta)$ between neighboring sites (see Fig. 1), with $c^{(\dagger)}_{x,\alpha}$ the annihilation (creation) operator of a fermion with flavor α at site x. The second, the Hubbard term, describes the on-site interaction between fermions with different flavors.

Interacting extensions of the SSH model have been used so far as a springboard to understand the effects of strong interactions, and have been concerned either with interacting bosonic [51–53], spinless fermionic models [54], or SU(2) fermionic models, i.e., with flavors associated with the $\uparrow$ ($\downarrow$) spin labels [26,54–56].

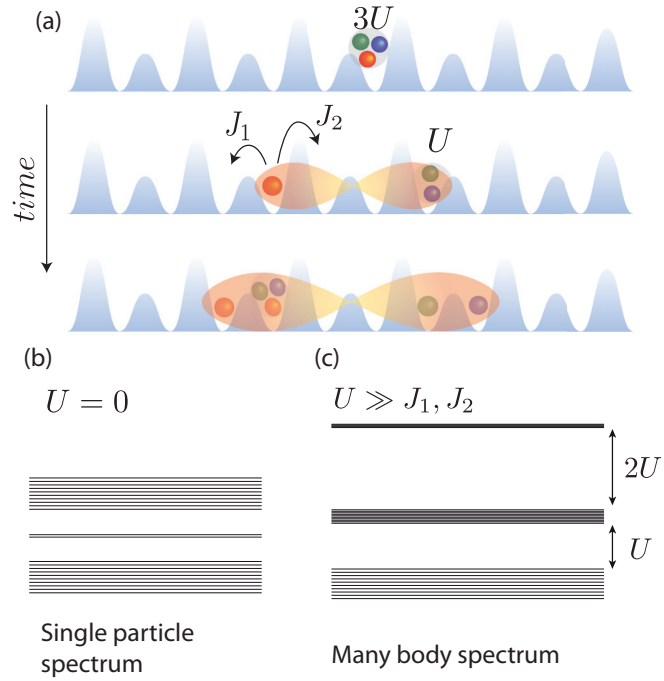

FIG. 1. (a) Multiparticle quantum walk on an SU(3) SSH lattice. U represents the strength of the on-site interaction. Three particles are injected at $t = 0$. The single- or multiparticle MCDs measured at later times provide information on the bulk states' topology. Here, $J_{1,2}$ represent the hoppings of the dimerized lattice, while U is the on-site repulsion energy. (b) Typical single-particle spectrum in the topological regime of the noninteracting spinless SSH model, with midgap lines indicating topological edge states. (c) Three-particle many-body spectrum of the SU(3) model for $U \gg J$. The spectrum consists of three bands separated by energy gaps of order $\sim U$.

In the absence of interactions, $U = 0$, the different flavor channels are decoupled and for $N = 3$ the model reduces to three copies of the noninteracting spinless SSH model [50]. The noninteracting model with $U = 0$ has an antiunitary chiral symmetry Γ, which transforms the local operators as $\Gamma c_{x,\alpha} \Gamma^{-1} \to (-1)^x c^\dagger_{x,\alpha}$ and $\Gamma\, i\, \Gamma^{-1} \to -i$ (see Supplemental Material [49] for details), and the model displays a topological phase transition at $\delta = 0$, from a trivial ($\delta < 0$) to a topologically nontrivial ($\delta > 0$) phase. The transition is characterized by a jump of π in the Zak phase [30]. A typical band structure for the spinless SSH model in the topological regime, with the zero-energy modes emphasized, is displayed in Fig. 1(b). The interacting Hamiltonian (1) also respects chiral symmetry apart from an overall chemical potential term, which is, however, irrelevant for the dynamics in a closed system, investigated here.

In the interacting model we find that excitations still exhibit two topological phases due to the presence of inversion symmetry, although zero-energy topologically protected edge excitations cease to exist. This is similar to the situation in noninteracting systems, where inversion symmetry enforces the Zak phase quantization, $\gamma_Z = 0$ or π (modulo 2π) [57]. This quantization has recently been demonstrated experimentally in a photonic lattice, where the chiral symmetry of a

noninteracting SSH model is broken by engineered long-range hopping, designed to preserve inversion symmetry [58].

To explore the topology of excitations, we inject three particles into the empty lattice in the middle of the chain by the three-particle creation operator $\Phi_x^{(3)\dagger} = \prod_{\alpha=1}^{3} c_{x,\alpha}^{\dagger}$, and investigate the effect of interactions in the quench dynamics in a multiparticle quantum walk setup [59–61], where the wave function follows a unitary evolution $|\Psi(t)\rangle = e^{-iHt}|\Psi(t=0)\rangle$ [see Fig. 1(a)].

B. Effective model for trions

Before investigating the quench dynamics, let us discuss shortly the many-body "band structure" of the Hamiltonian (1). A sketch of this band structure is displayed for $N = 3$ in Fig. 1(c) in the limit of strong interactions, $U \gg J$. The lowest band is constructed from states of propagating single fermions, and has a width $W_1 \approx 4J$. The highest in energy band, the trionic band, is constructed from states in which all the three particles reside mostly at the same site [62]. This band consists of L states (split into two subbands, as we show below), with very large energies $\approx 3U$, and a small bandwidth, of the order $W_3 \approx J^3/U^2$. Between the single-particle and the trionic bands there is the doublonic band, well separated in energy from the others. The average energy of doublons is of the order $\sim U$ (see Ref. [63] and the Supplemental Material [49] for more details on the band structure).

The initial state $|\Psi(0)\rangle = \Phi_x^{(3)\dagger}|0\rangle$ has an energy $\approx 3U$, and has most of its weight in the trionic band. In the large U limit, trions propagate across the lattice by high-order tunneling processes, and their dynamics is described by the effective Hamiltonian,

$$H_3 = \sum_x \Big\{ J_3[1 + \delta_3(-1)^x]\big(\tilde{\Phi}_x^{(3)\dagger}\tilde{\Phi}_{x+1}^{(3)} + \text{H.c.}\big) + E_3\tilde{\Phi}_x^{(3)\dagger}\tilde{\Phi}_x^{(3)}\Big\}, \tag{2}$$

where the $\tilde{\Phi}^{(3)\dagger}$ create dressed trion states, and E_3 and J_3 are the effective on-site energy and hopping, describing the trionic band [64]. The effective Hamiltonian (2) preserves the bipartite nature of the original Hamiltonian (1) with an effective dimerization δ_3 of the same order of magnitude as δ [49]. Trions are extremely heavy objects, and propagate through the lattice with a small effective velocity $v_3 \approx 2J_3 \ll v_1$, much smaller than the single-particle speed of propagation, $v_1 = 2J(1 - |\delta|)$. The initial three-particle state $\Phi_x^{(3)\dagger}|0\rangle$ overlaps with a large probability $p_3 \approx 1$ with the dressed trionic state, $\tilde{\Phi}_x^{(3)\dagger}|0\rangle$. It contains, however, with a small probability $p_2 \approx \frac{3}{2}J^2/U^2$ an admixture of doublons and free fermions, and an even smaller contribution from three independent fermions. Although they have a small contribution, these latter components propagate fast compared to trions.

III. TOPOLOGICAL TRANSITIONS IN THE INTERACTING SU(3) SSH MODEL

A. Many-body Berry phase

A numerical analysis performed by computing the winding number using the Green's functions for the SU($N = 2$) version of the model (1) at half filling indicates that interactions do not destroy the topology, although the bulk-boundary correspondence no longer survives [55]. Similar conclusions have been drawn from the analysis of two-body physics in spinless bosonic SSH models [51,52].

We now investigate the bulk properties of SU(3) SSH systems using the many-body Berry phase γ_B. We compute γ_B by using an approach, where in contrast to the standard methods [21,65–67], we determine the Berry phase over a *subset* of excited many-body states instead of simply using the ground state. The justification to use such a subset is that the initial three-particle state is built out of highly excited eigenstates. We consider a ring geometry, and impose twisted boundary conditions on the many-body spectrum. This is done by modifying one of the hopping terms $J \to Je^{i\theta_n}$ with $\theta_n = 2\pi n/M$, $n \in \{0, 1, \ldots, M-1\}$, and M controlling the twist angle discretization. For each θ_n, we diagonalize the Hamiltonian (1) within the $N = 3$ subspace, $H(\theta_n)\Psi_j^{(n)} = E_j^{(n)}\Psi_j^{(n)}$, and obtain the full many-body spectrum $\{E_j^{(n)}\}$ of the Hamiltonian.

The many-body Berry phase is well defined over a subset $\{\Psi_j\}$ of the many-body spectrum, separated by a gap from the rest of the states for all twist angles. By generalizing the procedure used for the ground state [21,65,67–69], we obtain

$$\gamma_B = -\text{Im}\log\prod_{n=0}^{M-1}\det[S^{(n,n+1)}], \tag{3}$$

where the elements of the matrix $S^{(n,n+1)}$ are

$$S_{jj'}^{(n,n+1)} = \big\langle\Psi_j^{(n)}\big|e^{2\pi iX/ML}\big|\Psi_{j'}^{(n+1)}\big\rangle, \tag{4}$$

with j, j' indexing the subset of many-body states, $\{\Psi_j\}$, and with $X = \sum_{j,\alpha} x\, c_{x,\alpha}^{\dagger}c_{x,\alpha}$ the many-body position operator along the chain. Under inversion symmetry the Berry phase transforms as $\gamma_B \to -\gamma_B$ (modulo 2π). Therefore, even in the interacting system, inversion symmetry enforces $\gamma_B = 0$ or π.

As explained earlier, the initial three-particle state is mainly constructed from states within the trionic band, which contains L states divided into two subbands, separated by a gap generated by the effective dimerization parameter δ_3. By including the $L/2$ highest-energy many-body states into the set $\{\Psi_j\}$, we recover a jump of π in γ_B at $\delta = 0$ (see Fig. 2). This indicates a topological phase transition between two topologically distinct regions, $\delta \lessgtr 0$.

B. Single- and many-body mean chiral displacements

The mean chiral displacement represents a dynamical measure capable to distinguish between the topological and the trivial regimes [27], defined as

$$\mathcal{P}_1(t) = \sum_x \langle\Psi(t)|(x - x_0)\Gamma\, n(x)|\Psi(t)\rangle. \tag{5}$$

Here, $p(x) = (x - x_0)n(x)$ denotes the regular polarization operator with respect to the reference point x_0 and by using the chiral-symmetry operator Γ, distinguishing between different sublattices, the "chiral polarization" operator or MCD is $(x - x_0)\Gamma n(x)$. $|\Psi(t)\rangle$ is the wave function time evolved from an appropriate initial state, localized on site x_0, now set as the middle of the chain [46]. Although $\mathcal{P}_1(t)$ depends on time, for noninteracting systems it converges to $\mathcal{P}_1(t \to \infty) \simeq \nu/2$,

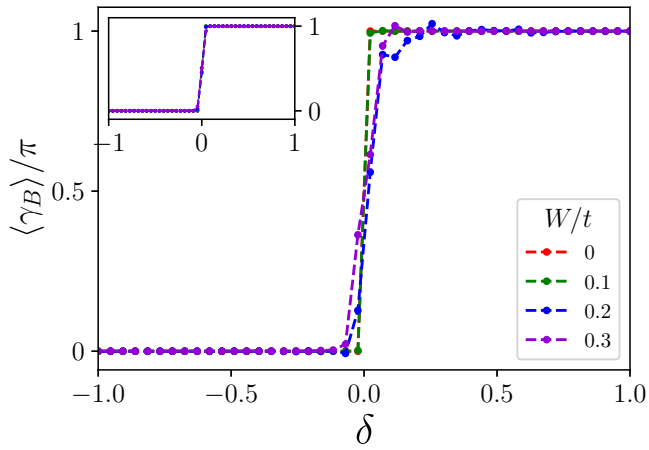

FIG. 2. Berry phase γ_B as a function of δ, obtained by integrating half of the excited (trion) many-body states in an $L = 8$ lattice with twisted boundary conditions, with $M = 20$ and $U = 3J$, for different chiral disorder strengths W. For each $W \neq 0$, we average over 100 disorder realizations. Inset: Berry phase for the noninteracting SSH model with hopping disorder

where ν is the bulk topological invariant associated with the Zak phase (see Supplemental Material [49] for a derivation).

Since the many-body state is mainly constructed from states in the trionic band, it is natural to extend the definition of the noninteracting MCD in Eq. (5), and introduce the many-body MCDs as

$$\mathcal{P}_3(t) \equiv \frac{1}{\langle n_3(t)\rangle}\langle\Psi(t)|\sum_x (-1)^x\, x\, \Phi_x^{(3)\dagger}\Phi_x^{(3)}|\Psi(t)\rangle. \quad (6)$$

The prefactor $\langle n_3(t)\rangle \leqslant 1$ measures the probability of three-particle occupation, $\langle n_3(t)\rangle = \sum_x \langle\Psi(t)|\,\Phi_3^\dagger(x)\Phi_3(x)|\Psi(t)\rangle$ [70]. Simple perturbation theory in J yields the asymptotic estimate, $\langle n_3(t\to\infty)\rangle \sim 1 - O(J^2/U^2)$. The results for γ_B are corroborated by the single-particle and the many-body MCDs, $\mathcal{P}_{1,3}(t)$, computed using both exact diagonalization and time evolving block decimation (TEBD) [71]. To tame the time oscillations, we also investigate the cumulative average MCDs, $\mathcal{P}^c_{1,3}(t) = \int_0^t \mathcal{P}_{1,3}(t')dt'/t$. Notice that $\mathcal{P}_{1,3}(t)$ are measures of the bulk topology, and do not provide any information on the localized states at the edges. Boundaries produce spurious artifacts while measuring $\mathcal{P}_{1,3}(t)$, they reflect propagating fronts, and yield boundary-induced oscillations in the simulations. The measurement time t_∞ is therefore always set to be smaller in our simulations than the time required for the front to reach the system boundaries.

The MCDs $\mathcal{P}_{1,3}(t)$ are presented in Fig. 3. The two insets in Fig. 3(a) display the time evolution of $\mathcal{P}_3(t)$ in the two regimes, as computed with TEBD. The asymptotic limit $\mathcal{P}_3(t_\infty)$ depends on the value of δ, and it converges to 0 (0.5) in the trivial (topological) regime. The main panel shows the δ dependence of the asymptotic values. The small oscillations in the asymptotic values are due to finite-size effects and limited simulation runtime, and they reduce in amplitude with increasing system size. As clear from Fig. 3, the many-body and the single-particle MCDs are both suitable tools to differentiate between topologically distinct regions. We also demonstrate [49] that both MCDs remain reasonably well quantized even away from the strongly correlated region as well.

C. Disorder effects

The quantization of the MCD is relatively robust against disorder. We have tested this robustness against different kinds of disorder. We have introduced a moderate *chiral* (hopping) disorder W breaking the inversion symmetry to test the robustness of γ_B. Figure 2 displays the results for γ_B for different W's. Although the jump at the transition becomes somewhat smeared, γ_B remains quantized as long as $W \lesssim \delta_3 \propto \delta$.

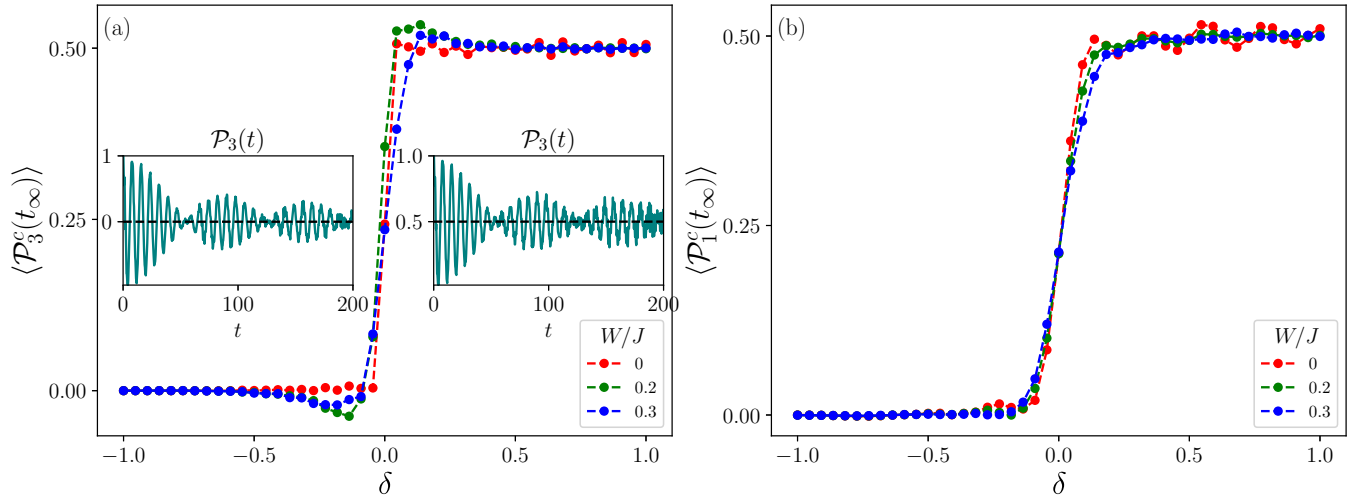

FIG. 3. Mean chiral displacement in the interacting $SU(3)$ SSH model. (a) Cumulative average MCD $\mathcal{P}_3^c$ for different chiral-symmetry preserving disorder strengths W as a function of dimerization parameter δ, for lattice size $L = 30$, and $t_\infty = 40/J$. Insets: Typical evolution of the MCD $\mathcal{P}_3$ in the clean system at (right) $\delta = 0.5$ and (left) $\delta = -0.5$. (b) Cumulative disorder-averaged MCD $\mathcal{P}_1^c$ for different disorder amplitudes as a function of dimerization parameter δ, for $L = 40$, and $t_\infty = 20/J$. In both panels $U = 3J$, and the average is done over 100 disorder realizations at each W.

Similarly, disorder does not affect significantly either $\mathcal{P}_1(t_\infty)$ or $\mathcal{P}_3(t_\infty)$, and the MCDs remain robust as well against the on-site or hopping disorder, as long as disorder is small compared to the topological gap for the excitations (see Fig. 3). Although moderate disorder does not destroy the topological band of excitations, strong interactions reduce the trion bandwidth as $\sim J^3/U^2$, and topological trion excitations become more susceptible to disorder in the limit of strong interactions (see Supplemental Material [49]).

D. Extension to the SU(N) SSH model

For clarity, so far we mostly focused on the SU(3) SSH model. Many of the results carry over, however, to the general SU(N) case. In the latter case, the N-particle many-body spectrum has a ladderlike structure with N bands, separated by energy gaps of the order of U. The highest in energy band, the N-ion band, has an energy $E_N \approx N(N-1)U/2$. The construction of the effective model that describes the N-ionic band, similar to Eq. (2) for the trions, is detailed in the Supplemental Material [49] and Ref. [63]. Computing the many-body Berry phase and the polarization is done along the same lines as for SU(3). Introducing the N-particle creation operator, $\Phi_x^{(N)} = \prod_{\alpha=1}^{N} c_{x,\alpha}^\dagger$, the many-body MCD is obtained as in Eq. (6) with the substitution $3 \to N$. Details for the Berry phase and MCD in the $SU(2)$ case are presented in the Supplemental Material [49]. Our findings also carry over to the case when *several* trions are injected to the lattice. We performed calculations for the case where two trions have been injected, and our findings [49] indicate that, irrespective of the strong interaction between trions, the MCDs $\mathcal{P}_{1,3}(t_\infty)$ remain unaffected in the long-time limit, and capture correctly the topological transition.

E. Connection to experiments

Experimental implementation of repulsive bound pairs has been realized by loading ^{87}Rb atoms in an optical lattice [72], while later on, the same setup was used to probe the dynamics and equilibrium properties of the topological SSH model [73]. In a state-of-the-art experiment [74], the SU($N > 2$) Fermi-Hubbard (FH) model has been realized by using ^{173}Yb atoms. By adjusting the lattice depth, one can tune the parameters of the FH model in the range $U/J \simeq 0.025$–2.5, confirming that our simulations are well within experimental reach. Experimentally, the three-body losses may become an important factor. The ratio of the on-site interaction and the three-body loss rate γ is found to scale as $U/\gamma h \propto (\lambda/a_s)^3$ for $N = 3$, where the scattering length for ^{173}Yb, $a_s \approx 10$ nm is much shorter than the wavelength $\lambda = 759$ nm of the confining laser [74]. In this system, for an interaction strength $U/J = 1$, we obtain the estimate $U/h \approx J/h \approx 300$ Hz, while the three-body loss rate is only $\gamma \approx 0.16$ Hz $\ll J/h$. The timescale of the three-body losses is at least one order or magnitude larger than the measurement time t_∞ of the experiment. The three-particle occupation defined in Eq. (6) can be measured by means of quantum gas microscopy, by extending the method of measuring two-particle occupations [75,76]. This is, however, not necessary in the strongly interacting regime, where $\langle n_3(t)\rangle$ is almost unity, as discussed above.

IV. CONCLUSIONS

We have investigated the quench dynamics in a multiparticle continuous-time quantum walk, and evaluated the effect of strong interactions on the topological properties of bulk excited states in the SU(3) SSH model. Strong interactions generically violate the conventional chiral symmetry of SSH models, nevertheless, a quantized many-body Berry phase is observed in the presence of inversion symmetry, signaling two distinct topological phases, separated by a π jump. The many-body topological phases are robust against moderate disorder. A similar discontinuity shows up in the asymptotic value of single-particle and many-body mean chiral displacements. Measuring the latter quantities in multiparticle quantum walk setups is within experimental reach, and could be used to infer the topological properties of the excited states. Similar features are expected for general SU(N) models as well.

ACKNOWLEDGMENTS

This research is supported by UEFISCDI, under Project No. PN-III-P4-ID-PCE-2020-0277, under the project for funding the excellence, Contracts No. 29 PFE/30.12.2021, No. PN-III-P1-1.1-PD-2019-0595, and No. PN-III-P1-1.1-TE-2019-0423, by the Core Program of the National Institute of Materials Physics, granted by the Romanian MCID under Project No. PC2-PN23080202, and by the National Research, Development and Innovation Office NKFIH within the Quantum Technology National Excellence Program (Project No. 2017-1.2.1-NKP-2017-00001), K134437, K142179, SNN139581, and the BME-Nanotechnology FIKP grant (BME FIKP-NAT). M.A.W. has also been supported by the Hungarian Academy of Sciences through the János Bolyai Research Scholarship and by the NKP-22-5-BME-330 New National Excellence Program of the Ministry for Culture and Innovation from the source of the National Research, Development and Innovation Fund.

[1] L. D. Landau and E. Lifshitz, *Statistical Physics*, Course of Theoretical Physics Vol. 5 (Butterworth-Heinemann, Oxford, U.K., 1980).
[2] M. Z. Hasan and C. L. Kane, Rev. Mod. Phys. **82**, 3045 (2010).
[3] X.-L. Qi and S.-C. Zhang, Rev. Mod. Phys. **83**, 1057 (2011).
[4] A. Y. Kitaev, in *Advances in Theoretical Physics: Landau Memorial Conference*, edited by V. Lebedev and M. Feigel'man, AIP Conf. Proc. No. 1134 (AIP, Melville, NY, 2009), p. 22.
[5] C.-K. Chiu, J. C. Y. Teo, A. P. Schnyder, and S. Ryu, Rev. Mod. Phys. **88**, 035005 (2016).
[6] A. M. Essin and V. Gurarie, Phys. Rev. B **84**, 125132 (2011).
[7] E. Prodan and H. Schulz-Baldes, *Bulk and Boundary Invariants for Complex Topological Insulators: From K-Theory to Physics* (Springer, Berlin, 2018).

[8] J. Alicea, Y. Oreg, G. Refael, F. von Oppen, and M. P. A. Fisher, Nat. Phys. **7**, 412 (2011).

[9] L. Šmejkal, Y. Mokrousov, B. Yan, and A. H. MacDonald, Nat. Phys. **14**, 242 (2018).

[10] Q. L. He, T. L. Hughes, N. P. Armitage, Y. Tokura, and K. L. Wang, Nat. Mater. **21**, 15 (2022).

[11] C. Wang, A. C. Potter, and T. Senthil, Science **343**, 629 (2014).

[12] S. Rachel, Rep. Prog. Phys. **81**, 116501 (2018).

[13] V. Gurarie, Phys. Rev. B **83**, 085426 (2011).

[14] K. Sun, H. Yao, E. Fradkin, and S. A. Kivelson, Phys. Rev. Lett. **103**, 046811 (2009).

[15] O. Vafek and K. Yang, Phys. Rev. B **81**, 041401(R) (2010).

[16] S. Raghu, X.-L. Qi, C. Honerkamp, and S.-C. Zhang, Phys. Rev. Lett. **100**, 156401 (2008).

[17] E. V. Castro, A. G. Grushin, B. Valenzuela, M. A. H. Vozmediano, A. Cortijo, and F. de Juan, Phys. Rev. Lett. **107**, 106402 (2011).

[18] I. F. Herbut, Phys. Rev. B **78**, 205433 (2008).

[19] A. W. W. Ludwig, Phys. Scr. **T168**, 014001 (2016).

[20] M. V. Berry, Proc. Math. Phys. Eng. Sci. **392**, 45 (1984).

[21] R. Resta, J. Phys.: Condens. Matter **12**, R107 (2000).

[22] D. Xiao, M.-C. Chang, and Q. Niu, Rev. Mod. Phys. **82**, 1959 (2010).

[23] D. Vanderbilt, *Berry Phases in Electronic Structure Theory: Electric Polarization, Orbital Magnetization and Topological Insulators* (Cambridge University Press, Cambridge, U.K., 2018).

[24] F. Pollmann, A. M. Turner, E. Berg, and M. Oshikawa, Phys. Rev. B **81**, 064439 (2010).

[25] P. Fromholz, G. Magnifico, V. Vitale, T. Mendes-Santos, and M. Dalmonte, Phys. Rev. B **101**, 085136 (2020).

[26] D. Wang, S. Xu, Y. Wang, and C. Wu, Phys. Rev. B **91**, 115118 (2015).

[27] F. Cardano, A. DErrico, A. Dauphin, M. Maffei, B. Piccirillo, C. de Lisio, G. De Filippis, V. Cataudella, E. Santamato, L. Marrucci, M. Lewenstein, and P. Massignan, Nat. Commun. **8**, 15516 (2017).

[28] T. Kitagawa, M. A. Broome, A. Fedrizzi, M. S. Rudner, E. Berg, I. Kassal, A. Aspuru-Guzik, E. Demler, and A. G. White, Nat. Commun. **3**, 882 (2012).

[29] T. Groh, S. Brakhane, W. Alt, D. Meschede, J. K. Asbóth, and A. Alberti, Phys. Rev. A **94**, 013620 (2016).

[30] M. Atala, M. Aidelsburger, J. T. Barreiro, D. Abanin, T. Kitagawa, E. Demler, and I. Bloch, Nat. Phys. **9**, 795 (2013).

[31] E. J. Meier, F. A. An, A. Dauphin, M. Maffei, P. Massignan, T. L. Hughes, and B. Gadway, Science **362**, 929 (2018).

[32] Y. Wang, Y.-H. Lu, F. Mei, J. Gao, Z.-M. Li, H. Tang, S.-L. Zhu, S. Jia, and X.-M. Jin, Phys. Rev. Lett. **122**, 193903 (2019).

[33] T. Rakovszky, J. K. Asbóth, and A. Alberti, Phys. Rev. B **95**, 201407(R) (2017).

[34] X. Zhan, L. Xiao, Z. Bian, K. Wang, X. Qiu, B. C. Sanders, W. Yi, and P. Xue, Phys. Rev. Lett. **119**, 130501 (2017).

[35] H. Schmitz, R. Matjeschk, C. Schneider, J. Glueckert, M. Enderlein, T. Huber, and T. Schaetz, Phys. Rev. Lett. **103**, 090504 (2009).

[36] M. Karski, L. Förster, J.-M. Choi, A. Steffen, W. Alt, D. Meschede, and A. Widera, Science **325**, 174 (2009).

[37] A. Peruzzo, M. Lobino, J. C. F. Matthews, N. Matsuda, A. Politi, K. Poulios, X.-Q. Zhou, Y. Lahini, N. Ismail, K. Wörhoff, Y. Bromberg, Y. Silberberg, M. G. Thompson, and J. L. OBrien, Science **329**, 1500 (2010).

[38] A. Schreiber, K. N. Cassemiro, V. Potoček, A. Gábris, P. J. Mosley, E. Andersson, I. Jex, and C. Silberhorn, Phys. Rev. Lett. **104**, 050502 (2010).

[39] K. Poulios, R. Keil, D. Fry, J. D. A. Meinecke, J. C. F. Matthews, A. Politi, M. Lobino, M. Gräfe, M. Heinrich, S. Nolte, A. Szameit, and J. L. O'Brien, Phys. Rev. Lett. **112**, 143604 (2014).

[40] T. Fukuhara, P. Schauß, M. Endres, S. Hild, M. Cheneau, I. Bloch, and C. Gross, Nature (London) **502**, 76 (2013).

[41] T. Fukuhara, A. Kantian, M. Endres, M. Cheneau, P. Schauß, S. Hild, D. Bellem, U. Schollwöck, T. Giamarchi, C. Gross, I. Bloch, and S. Kuhr, Nat. Phys. **9**, 235 (2013).

[42] L. Lu, J. D. Joannopoulos, and M. Soljai, Nat. Photonics **8**, 821 (2014).

[43] T. Ozawa, H. M. Price, A. Amo, N. Goldman, M. Hafezi, L. Lu, M. C. Rechtsman, D. Schuster, J. Simon, O. Zilberberg, and I. Carusotto, Rev. Mod. Phys. **91**, 015006 (2019).

[44] P. M. Preiss, R. Ma, M. E. Tai, A. Lukin, M. Rispoli, P. Zupancic, Y. Lahini, R. Islam, and M. Greiner, Science **347**, 1229 (2015).

[45] Z. A. Geiger, K. M. Fujiwara, K. Singh, R. Senaratne, S. V. Rajagopal, M. Lipatov, T. Shimasaki, R. Driben, V. V. Konotop, T. Meier, and D. M. Weld, Phys. Rev. Lett. **120**, 213201 (2018).

[46] A. Haller, P. Massignan, and M. Rizzi, Phys. Rev. Res. **2**, 033200 (2020).

[47] F. Haldane, Phys. Lett. A **93**, 464 (1983).

[48] R. Verresen, R. Moessner, and F. Pollmann, Phys. Rev. B **96**, 165124 (2017).

[49] See Supplemental Material at http://link.aps.org/supplemental/10.1103/PhysRevB.108.035126 for details on the derivation of SU(N) effective models at large interaction strength U. It performs additional numerical investigations of many-body Berry phase and MCD in SU(2) and SU(3) models. Also it investigates briefly the case of two trions interacting in the SSH lattice.

[50] W. P. Su, J. R. Schrieffer, and A. J. Heeger, Phys. Rev. Lett. **42**, 1698 (1979).

[51] M. Di Liberto, A. Recati, I. Carusotto, and C. Menotti, Phys. Rev. A **94**, 062704 (2016).

[52] M. A. Gorlach and A. N. Poddubny, Phys. Rev. A **95**, 053866 (2017).

[53] A. A. Stepanenko and M. A. Gorlach, Phys. Rev. A **102**, 013510 (2020).

[54] J. Sirker, M. Maiti, N. P. Konstantinidis, and N. Sedlmayr, J. Stat. Mech.: Theory Exp. **2014**, P10032 (2014).

[55] S. R. Manmana, A. M. Essin, R. M. Noack, and V. Gurarie, Phys. Rev. B **86**, 205119 (2012).

[56] N. H. Le, A. J. Fisher, N. J. Curson, and E. Ginossar, npj Quantum Inf. **6**, 24 (2020).

[57] J. Zak, Phys. Rev. Lett. **62**, 2747 (1989).

[58] Z.-Q. Jiao, S. Longhi, X.-W. Wang, J. Gao, W.-H. Zhou, Y. Wang, Y.-X. Fu, L. Wang, R.-J. Ren, L.-F. Qiao, and X.-M. Jin, Phys. Rev. Lett. **127**, 147401 (2021).

[59] Y. Aharonov, L. Davidovich, and N. Zagury, Phys. Rev. A **48**, 1687 (1993).

[60] E. Farhi and S. Gutmann, Phys. Rev. A **58**, 915 (1998).

[61] A. M. Childs, E. Farhi, and S. Gutmann, Quantum Inf. Process. **1**, 35 (2002).

[62] Trion states are defined as three-particle eigenstates of the interacting Hamiltonian, adiabatically connected to the three-particle states in the $J \to 0$ limit. Doublons are defined similarly, as two-particle eigenstates.
[63] M. A. Werner, C. P. Moca, M. Kormos, Ö. Legeza, B. Dóra, and G. Zaránd, arXiv:2207.00994.
[64] The operators $\tilde{\Phi}_x^{(3)\dagger}$ and $\Phi_x^{(3)\dagger}$ should not be confused, as the first one creates a dressed trion state while the second one is a three-particle creation operator at position x.
[65] R. Resta and S. Sorella, Phys. Rev. Lett. **74**, 4738 (1995).
[66] G. Ortiz, P. Ordejón, R. M. Martin, and G. Chiappe, Phys. Rev. B **54**, 13515 (1996).
[67] R. Resta and S. Sorella, Phys. Rev. Lett. **82**, 370 (1999).
[68] R. Resta, Phys. Rev. Lett. **80**, 1800 (1998).
[69] A. A. Aligia and G. Ortiz, Phys. Rev. Lett. **82**, 2560 (1999).
[70] In Eq. (6) the reference point is the set to the middle of the chain and corresponds to $x_0 = 0$.
[71] G. Vidal, Phys. Rev. Lett. **98**, 070201 (2007).
[72] K. Winkler, G. Thalhammer, F. Lang, R. Grimm, J. Hecker Denschlag, A. J. Daley, A. Kantian, H. P. Büchler, and P. Zoller, Nature (London) **441**, 853 (2006).
[73] E. J. Meier, F. A. An, and B. Gadway, Nat. Commun. **7**, 13986 (2016).
[74] C. Hofrichter, L. Riegger, F. Scazza, M. Höfer, D. R. Fernandes, I. Bloch, and S. Fölling, Phys. Rev. X **6**, 021030 (2016).
[75] T. Hartke, B. Oreg, N. Jia, and M. Zwierlein, Phys. Rev. Lett. **125**, 113601 (2020).
[76] D. Mitra, P. T. Brown, E. Guardado-Sanchez, S. S. Kondov, T. Devakul, D. A. Huse, P. Schauß, and W. S. Bakr, Nat. Phys. **14**, 173 (2018).